Hierarchical and Safe Motion Control for Cooperative Locomotion of Robotic Guide Dogs and Humans: A Hybrid Systems Approach

Kaveh Akbari Hamed[1], Vinay R. Kamidi[1], Wen-Loong Ma[2], Alexander Leonessa[1], and Aaron D. Ames[2]

***Abstract*—This paper presents a hierarchical control strategy based on hybrid systems theory, nonlinear control, and safety-critical systems to enable cooperative locomotion of robotic guide dogs and visually impaired people. We address high-dimensional and complex hybrid dynamical models that represent collaborative locomotion. At the high level of the control scheme, local and nonlinear controllers, based on the virtual constraints approach, are designed to induce exponentially stable dynamic gaits. The local controller for the leash is assumed to be a nonlinear controller that keeps the human in a safe distance from the dog while following it. At the lower level, a real-time quadratic programming (QP) is solved for modifying the local controllers of the robot as well as the leash to avoid obstacles. In particular, the QP framework is set up based on control barrier functions (CBFs) to compute optimal control inputs that guarantee safety while being close to the local controllers. The stability of the complex periodic gaits is investigated through the Poincaré return map. To demonstrate the power of the analytical foundation, the control algorithms are transferred into an extensive numerical simulation of a complex model that represents cooperative locomotion of a quadrupedal robot, referred to as Vision 60, and a human model. The complex model has 16 continuous-time domains with 60 state variables and 20 control inputs.**

***Index Terms*—Legged Robots, Motion Control, Dynamics**

I. INTRODUCTION

THIS paper aims to develop an analytical foundation, based on hybrid systems theory, nonlinear control, quadratic programming, and safety-critical systems, to develop a hierarchical control algorithm that enables safe and stable cooperative locomotion of robotic guide dogs and visually impaired people (see Fig. 1). According to [1], most of the impaired people mainly rely on their useable vision, a guide dog, or a sighted guide rather than using white canes. Although dogs are very smart animals with an outstanding level of cooperation with people, behavioural traits such as trainability, reactivity or attention to environmental stimuli, and level of aggressiveness are of concern to some owners [2]. State-of-the-art approaches to improve the quality of life for the visually impaired are tailored to the navigation techniques via GPS and smartphone applications (e.g., [3], [4], [5]) and neglect mobility. It is to be noted that the difference between navigation and mobility lies in the fact that navigation systems point out obstacles/hindrances but mobility systems show the way around. This together with the fact that more than half the Earth's landmass is inaccessible to wheeled vehicles motivates the development of autonomous *legged guide robots* that cooperatively work with visually impaired people in human-centered communities.

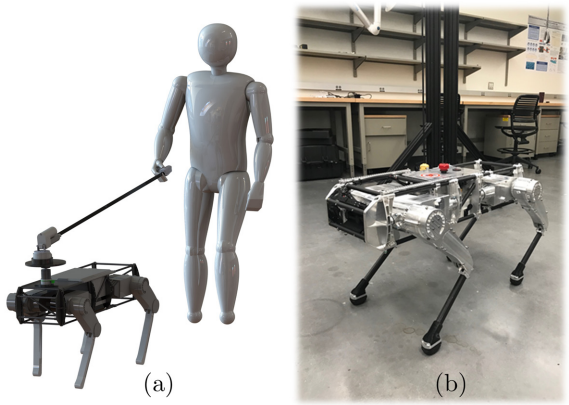

Fig. 1: (a) Illustration of a visually impaired human being guided by a quadrupedal assistance robot. (b) Vision 60 robot manufactured by Ghost Robotics [6] whose full-order hybrid model will be used for the numerical simulations.

Related Work: Although important theoretical and technological advances have occurred for the construction and control of guide robots, state-of-the-art approaches are mainly tailored to the deployment of wheeled vehicles and *not* legged guide robots (e.g., [7], [8], [9]). Unlike wheeled guide robots, legged robots are *inherently unstable* complex dynamical systems with hybrid nature and high degrees of freedom (DOF). This complicates the design of feedback control algorithms that ensure stable and safe cooperative locomotion of guide dogs and human. Hybrid systems theory has become a powerful approach for the modeling and control of legged robots both in theory and practice [10], [11], [12], [13], [14], [15], [16], [17], [18], [19], [20], [21], [22], [23]. Existing control approaches

Manuscript received: April 4, 2019; Revised July 7, 2019; Accepted August 17, 2019.

This paper was recommended for publication by Editor Nikos Tsagarakis upon evaluation of the Associate Editor and Reviewers' comments. *The work of K. Akbari Hamed is supported by the National Science Foundation (NSF) under Grant Numbers 1854898, 1906727, 1923216, and 1924617. The work of V. R. Kamidi is supported by the NSF Grant Number 1854898. The work of A. D. Ames is supported by the NSF under Grant Numbers 1544332, 1724457, 1724464, 1923239, and 1924526 as well as Disney Research LA. The content is solely the responsibility of the authors and does not necessarily represent the official views of the NSF.

[1]K. Akbari Hamed, V. R. Kamidi, and A. Leonessa are with the Department of Mechanical Engineering, Virginia Tech, Blacksburg, VA 24061 USA kavehakbarihamed@vt.edu, vinay28@vt.edu and aleoness@vt.edu

[2]W. Ma and A. D. Ames are with the Department of Mechanical and Civil Engineering, California Institute of Technology, Pasadena, CA 91125 USA wma@caltech.edu and ames@cds.caltech.edu

Digital Object Identifier (DOI): see top of this page.

This article has been accepted for publication in a future issue of this journal, but has not been fully edited. Content may change prior to final publication. Citation information: DOI 10.1109/LRA.2019.2939719, IEEE Robotics and Automation Letters

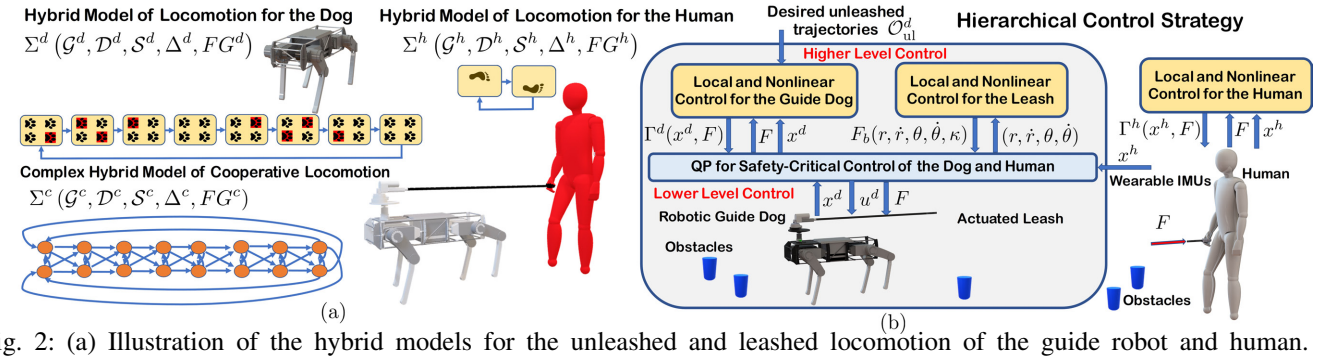

Fig. 2: (a) Illustration of the hybrid models for the unleashed and leashed locomotion of the guide robot and human. (b) Illustration of the proposed hierarchical control strategy for the safe and stable cooperative locomotion.

that address the hybrid nature of legged locomotion models are developed based on hybrid reduction [24], controlled symmetries [21], transverse linearization [22], and hybrid zero dynamics (HZD) [11], [13]. State-of-the art nonlinear control approaches for dynamic legged locomotion have been tailored to stable locomotion of legged robots, but *not* stable and safe cooperative locomotion of legged guide robots and visually impaired people.

Objectives and Contributions: The *objectives* and *contributions* of this paper are to present a formal foundation towards 1) developing complex hybrid models of cooperative locomotion of legged guide dogs and human, and 2) creating a hierarchical control algorithm, based on nonlinear control, quadratic programming, and control barrier functions (CBFs) [25], [26], [27], to ensure stability, safety, and obstacle avoidance. We address complex and high-dimensional models of cooperative legged locomotion via hybrid systems approach. An actuated leash structure is considered for the coordination of the dog and human locomotion while steering the human for safety and obstacle avoidance. At the higher level, the proposed hierarchical control algorithm employs local and nonlinear controllers that induce asymptotically stable unleashed locomotion patterns for the robotic dog and human. The local controllers are synthesized via the HZD approach and assumed to have access to the local state measurements as well as the force measurement applied by the leash structure. The leash local controller is then designed to keep the human in a safe distance from the robot while following it. The existence and stability of complex and leashed locomotion patterns for the coupled dynamics are addressed through the Poincaré return map. At the lower level of the control strategy, the local controllers for the dog and leash are modified by a real-time quadratic programming (QP) that includes CBF constraints to ensure safety and obstacle avoidance. The power of the anlytical results are demonstrated on an extensive numerical simulation of a complex hybrid model that represents cooperative locomotion of a quadrupedal robot, referred to as Vision 60 [6] (see Fig. 1), and a human model in the presence of a discrete set of obstacles. The proposed work is a departure form authors' previous work on HZD gait planning and control and CBFs in [28], [29], [30], [14], [25], [26], [27]. In particular, the previous work considers the motion planning and control of one legged agent. The current paper, however, addresses complex hybrid models of human-robot cooperative locomotion (two agents) and then develops hierarchical, distributed, and safe control algorithms for these sophisticated systems in the presence of obstacles. The work is also different from the solid analytical study presented in [31], [32], [33] for locomotion adaptation of limit cycle bipedal walkers in leader/follower collaborative tasks. More specifically, the current paper addresses modeling of two agents, their complex and coupled hybrid dynamics, and designing local and optimal controllers for stable locomotion and obstacle avoidance. References [31]-[33], however, consider the follower dynamics while designing a switching based controller for its adaptation to a persistent external force that represents the leader.

II. HYBRID MODELS OF LOCOMOTION

In this section, we will first present the hybrid models for the locomotion of each agent (i.e., robot and human). We will then address the complex hybrid model that describes the cooperative locomotion of agents. Throughout this paper, we shall consider *multi-domain* hybrid models described by the tuple $\Sigma\left(\mathcal{G},\mathcal{D},\mathcal{S},\Delta,FG\right)$ [28], where $\mathcal{G}:=(\mathcal{V},\mathcal{E})$ represents a *direct cycle* (i.e., graph) for the studied locomotion pattern (see Fig. 2a). In our formulation, the vertices $\mathcal{V}$ denote the continuous-time dynamics of legged locomotion, referred to as *domains* or *phases*. The edges $\mathcal{E}\subseteq\mathcal{V}\times\mathcal{V}$ represent the discrete-time transitions among continuous-time dynamics arising from changes in physical constraints. The state variables and control inputs of the hybrid system are shown by $x\in\mathcal{X}$ and $u\in\mathcal{U}$, respectively. The set of state manifolds and set of admissible controls are then denoted by $\mathcal{X}$ and $\mathcal{U}$. The set of domains of admissibility are further represented by $\mathcal{D}\subset\mathcal{X}\times\mathcal{U}$. The evolution of the hybrid system during the continuous-time domain $v\in\mathcal{V}$ is described by an ordinary differential equation (ODE) arising from the Euler-Lagrange equations as $\dot{x}=f_v(x)+g_v(x)\,u$. In addition, $FG:=\{(f_v,g_v)\}_{v\in\mathcal{V}}$ represents the set of control systems on $\mathcal{D}$. The evolution of the hybrid system during the discrete-time transition $e\in\mathcal{E}$ is further described by the instantaneous mapping $x^+=\Delta_e(x^-)$, where x^- and x^+ represent the state of the system right before and after the discrete transition, respectively. $\Delta:=\{\Delta_e\}_{e\in\mathcal{E}}$ denotes the set of discrete-time dynamics. The guards of the hybrid system are finally given by $\mathcal{S}:=\{\mathcal{S}_e\}_{e\in\mathcal{E}}$.

A. Hybrid Model for One Agent

Continuous-Time Dynamics: We assume that $q\in\mathcal{Q}\subset\mathbb{R}^n$ denotes the configuration variables for the robot and/or human.

This article has been accepted for publication in a future issue of this journal, but has not been fully edited. Content may change prior to final publication. Citation information: DOI 10.1109/LRA.2019.2939719, IEEE Robotics and Automation Letters

The configuration space is further represented by $\mathcal{Q}$. The state vector is taken as $x := \text{col}(q, \dot{q}) \in \text{T}\mathcal{Q}$. We remark that the Vision 60 has $n = 18$ DOFs. For the human model, we make use of an $n = 12$ DOF tree structure with a torso and two identical legs consisting of a femur and tibia links. The control inputs $u \in \mathcal{U} \subset \mathbb{R}^m$ are finally taken as torques at the joint levels (i.e., $m = 12$ for the robot and $m = 6$ for the human model). The equations of motion during the domain v are then described by the Euler-Lagrange equations and principle of virtual work as follows

$$\begin{aligned} D(q)\,\ddot{q} + C\,(q,\dot{q})\,\dot{q} + G(q) &= B\,u + J_v^{\top}(q)\,\lambda \\ J_v(q)\,\ddot{q} + \frac{\partial}{\partial q}\,(J_v(q)\,\dot{q})\,\dot{q} \quad &= 0, \end{aligned} \tag{1}$$

where $D(q) \in \mathbb{R}^{n\times n}$ denotes the positive definite mass-inertia matrix, $C(q,\dot{q})\,\dot{q} + G(q) \in \mathbb{R}^n$ represents the Coriolis, centrifugal, and gravitational terms, $B \in \mathbb{R}^{n\times m}$ denotes the input distribution matrix, λ represents the Lagrange multipliers (i.e., ground reaction forces), and $J_v(q)$ is the contact Jacobian matrix with the ground. If J_v has full rank, one can eliminate the Lagrange multipliers to express (1) as

$$D(q)\,\ddot{q} + H_v\,(q,\dot{q}) = T_v(q)\,u. \tag{2}$$

Discrete-Time Dynamics: If a new contact point is added to the existing set of contact points with the ground, we employ a rigid impact model [34] to describe the abrupt changes in the velocity coordinates according to the impact as $x^+ = \Delta_e(x^-)$ (see [28] for more details). Furthermore, if the leg leaves the ground, we take Δ_e as the identity map to preserve the continuity of states.

B. Complex Hybrid Models for Cooperative Locomotion

Throughout this paper, we shall assume that there is a rigid and massless leash model that connects a point on the dog (e.g., head) to a point on the human (e.g., hand or hip). The leash will further be assumed to be actuated to control its length and orientation so that the human can follow the dog in a safe manner. This will be clarified with more details in Section III-B.

Complex Graph: The state and control inputs for the robotic dog and human are shown by $x^i := \text{col}(q^i, \dot{q}^i)$ and u^i, respectively, for $i \in \{d, h\}$, where the superscripts "d" and "h" stand for the dog and human. The complex hybrid model that describes the cooperative locomotion of the robot and human will have a complex graph that is taken as the strong product of graphs $\mathcal{G}^d = (\mathcal{V}^d, \mathcal{E}^d)$ and $\mathcal{G}^h = (\mathcal{V}^h, \mathcal{E}^h)$. The strong product is denoted by $\mathcal{G}^c := \mathcal{G}^d \boxtimes \mathcal{G}^h$ that has the vertex set $\mathcal{V}^c := \mathcal{V}^d \times \mathcal{V}^h$, and any two vertices (v, w) and (v', w') in $\mathcal{V}^c$ are adjacent if and only if 1) $v = v'$ and $(w \to w')$ is an edge in $\mathcal{E}^h$, or 2) $(v \to v')$ is an edge in $\mathcal{E}^d$ and $w = w'$, or 3) $(v \to v')$ is an edge in $\mathcal{E}^d$ and $(w \to w')$ is an edge in $\mathcal{E}^h$. In our notation, the superscript "c" represents the complex model. The augmented state and control inputs are further denoted by $x^c := \text{col}(x^d, x^h)$ and $u^c := \text{col}(u^d, u^h)$, respectively.

Complex Continuous-Time Dynamics: For every vertex $(v, w) \in \mathcal{V}^c$, the evolution of the composite mechanical system, consisting of the robot and human, can be described by the following nonlinear and *coupled* dynamics

$$\begin{aligned} D^d\left(q^d\right)\ddot{q}^d + H_v^d\left(q^d, \dot{q}^d\right) &= T_v^d\left(q^d\right)u^d - J_{\text{head}}^{d\top}\left(q^d\right)F \\ D^h\left(q^h\right)\ddot{q}^h + H_w^h\left(q^h, \dot{q}^h\right) &= T_w^h\left(q^h\right)u^h + J_{\text{hand}}^{h\top}\left(q^h\right)F, \end{aligned} \tag{3}$$

in which $J_{\text{head}}^d(q^d)$ and $J_{\text{hand}}^h(q^h)$ denote the Jacobian matrices for the end points of the leash at the dog and human sides, respectively, and $F \in \mathbb{R}^3$ represents the force applied by the leash to the human hand.

Complex Discrete-Time Dynamics: Since the leash model is assumed to be massless and cannot employ impulsive forces, the evolution of the composite mechanical system over the discrete transition $(v, w) \to (v', w')$ can be described by the following nonlinear and *decoupled* mappings

$$x^{d+} = \Delta_{v\to v'}^d\left(x^{d-}\right), \quad x^{h+} = \Delta_{w\to w'}^h\left(x^{h-}\right). \tag{4}$$

We remark that if $v = v'$ (resp. $w = w'$) in (4), the mapping $\Delta_{v\to v'}$ (resp. $\Delta_{w\to w'}$) is simply taken as the identity.

***Remark** 1:* In this paper, we shall consider a trotting gait for Vision 60 robot with 8 continuous-time domains (see Fig. 2a for more details). The graph for the bipedal gait of the human model also has 2 continuous-time domains that represent the right and left stance phases. Consequently, the complex hybrid model of locomotion would have $8 \times 2 = 16$ continuous-time domains for which there are $2 \times (n^d + n^h) = 2 \times (18 + 12) = 60$ state variables and $m^d + m^h + m^l = 12 + 6 + 2 = 20$ control inputs. Here, $m^l = 2$ represents the actuator numbers for the leash (see Section III-B).

III. HIERARCHICAL CONTROL STRATEGY

In order to have stable and safe cooperative locomotion for the robot and human, we will present a two-level control strategy for the robotic dog and leash (see Fig. 2b). Since the mathematical models for the local controller of the human part are not known, we shall assume a nonlinear local controller for the human, but will *not* change that controller to address unforeseen events and obstacle avoidance. We will instead focus on the dog and leash hierarchical control strategy to ensure stability and safety. At the higher level of the control strategy, we will employ a local nonlinear controller for the robot that has access to its own state variables as well as the force employed by the leash (i.e., force measurement). This controller will be referred to as the *robot local controller*. The objective is to asymptotically derive some outputs to zero that encode the locomotion patterns for the guide robot. This controller exponentially stabilizes gaits for the hybrid model of the dog in the presence of the leash force. The local controller for the leash will be designed to ensure that 1) there is always a safe distance between the robot and human, and 2) human follows the robot (see Section III-B). At the lower level, we will solve a real-time QP optimization to modify the local controllers of the robot and leash to ensure safety and obstacle avoidance.

A. Local Controllers for the Agents

In this section, we consider the robot and human as two multi-body "agents" specified by the superscript $i \in \{d, h\}$.

***Definition** 1 (Local Controllers):* We suppose that there are local and smooth feedback laws $\Gamma^i(x^i, F) :=$

This article has been accepted for publication in a future issue of this journal, but has not been fully edited. Content may change prior to final publication. Citation information: DOI 10.1109/LRA.2019.2939719, IEEE Robotics and Automation Letters

$\{\Gamma_v^i(x^i, F)\}_{v\in\mathcal{V}^i}$ for agent $i \in \{d, h\}$ yielding stable locomotion patterns. In our notation, $\Gamma_v^i(x^i, F)$ is a local and nonlinear feedback controller that is employed during the continuous-time $v \in \mathcal{V}^i$ and assumed to have access to the state variables of the agent i as well as the force F.

***Assumption** 1 (Transvsersal Stable Periodic Orbits):* By employing the local controllers for the agent $i \in \{d, h\}$ in the unleashed case (i.e., $F \equiv 0$), we assume that there is a period-one gait for the closed-loop model Σ^i, denoted by $\mathcal{O}^i_{\text{ul}}$, that is transversal to the guards $\mathcal{S}^i$. In our notation, the subscript "ul" stands for the unleashed gait. The orbit $\mathcal{O}^i_{\text{ul}}$ is further supposed to be exponentially stable.

For future purposes, the evolution of the state variables x^i on the unleashed orbit $\mathcal{O}^i_{\text{ul}}$ is represented by $x^i_\star(t)$ for $t \geq 0$. The orbit $\mathcal{O}^i_{\text{ul}}$ can then be expressed as $\mathcal{O}^i_{\text{ul}} := \left\{x^i = x^i_\star(t) \,|\, 0 \leq t < T^i\right\}$, in which $T^i > 0$ denotes the minimal period of $x^i_\star(t)$.

***Assumption** 2 (Common Multiples of Gait Periods):* We assume that there are common multiples for the periods of the dog and human unleashed gaits. More specifically, there are positive integers N^d and N^h such that $N^d T^d = N^h T^h$. For future purposes, we denote the minimum of these values by $N^d_{\min}$ and $N^h_{\min}$.

Assumption 2 states conditions under which there is a periodic orbit for the unleashed and augmented hybrid model including the dog and human. If this condition is violated, the unleashed model may not have any periodic solution.

B. Leash Local Controller

Leash Structure: The leash structure is assumed to be rigid with 3 DOFs including the leash length and its orientation in the spherical coordinates as conceptually illustrated in Fig. 3. We denote the Cartesian coordinates of the leash ends on the robot's body and human hand by $p^d_{\text{head}}(q^d) \in \mathbb{R}^3$ and $p^h_{\text{hand}}(q^h) \in \mathbb{R}^3$, respectively. Next, we consider the vector connecting $p^h_{\text{hand}}(q^h)$ to $p^d_{\text{head}}(q^d)$. The representation of this vector in the spherical coordinates can be given by the joint variables (r, θ, ϕ) as shown in Fig. 3. We further suppose that r and θ can be controlled by linear and rotational actuators, respectively, whereas the angle ϕ is unactuated. There are linear and rotational encoders for the leash structure to measure (r, θ). In addition, it is supposed that the angle ϕ is very small and negligible for flat ground walking. A force cell is utilized in the design as shown Fig. 3 to measure the force applied by the leash structure on the dog dynamics. This will be used for the force feedback measurement of the robot's local controller as mentioned in Definition 1. The objective here is to design a local force feedback controller for the leash that has access to (r, θ) to keep the human in a safe distance from the robot dog while regulating the angle θ. In particular, we are interested in (i) having $r \in [r_{\min}, r_{\max}]$ for some $0 < r_{\min} < r_{\max}$ and (ii) imposing $\theta \to 0$. This controller is referred to as the *leash local controller*. One possible way to design such a controller is to decompose the force F into (F_r, F_θ, F_ϕ) (see Fig. 3), in which $F_r(r, \dot{r})$ is the longitudinal force to be zero over the safe zone $[r_{\min}, r_{\max}]$. Moreover, $F_\theta(\theta, \dot{\theta})$ is a torsional force that can be taken as a simple PD controller to regulate θ. F_ϕ is assumed to be zero. For

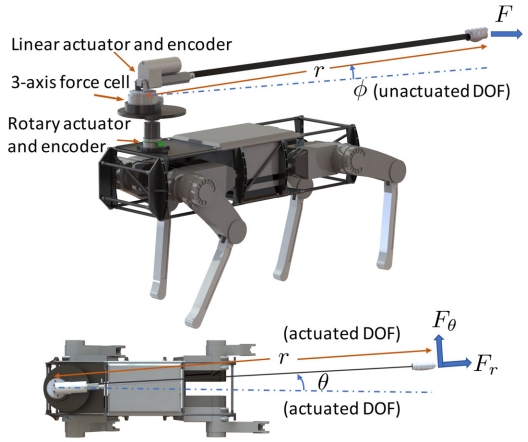

Fig. 3: Conceptual illustration of the leash structure.

future purposes, the leash local controller will be represented by $F_b(r, \dot{r}, \theta, \dot{\theta}, \kappa) \in \mathbb{R}^3$, where κ represents some adjustable controller parameters, e.g., PD gains.

***Assumption** 3:* We assume that F_b is sufficiently differentiable with respect to its arguments $(r, \dot{r}, \theta, \dot{\theta}, \kappa)$. This would help us to carry out the exponential stability analysis in Theorem 1. Furthermore, for $\kappa = 0$, $F_b(r, \dot{r}, \theta, \dot{\theta}, \kappa) \equiv 0$.

***Example** 1:* One typical example for the longitudinal force $F_r(r, \dot{r})$ can be given by a discontinuous and piecewise-defined function as $F_r(r, \dot{r}) = -(k_r(r - r_{\min}) + b_r\dot{r})\,1(r_{\min} - r) - (k_r(r - r_{\max}) + b_r\dot{r})\,1(r - r_{\max})$, which is zero over $[r_{\min}, r_{\max}]$. Here, $1(\cdot)$ is the step function and k_r and b_r are some positive gains. By approximating the step function by $1(r) \approx \varphi(r) := \frac{1}{1+\exp(-r/\epsilon)}$ for some $0 < \epsilon \ll 1$, one can obtain a smooth version of this longitudinal force. The torsional force can be then taken as $F_\theta(\theta, \dot{\theta}) := -k_\theta\,\theta - b_\theta\,\dot{\theta}$. The leash controllers is finally represented by $F_b(r, \dot{r}, \theta, \dot{\theta}, \kappa)$ with $\kappa := \text{col}(k_r, b_r, k_\theta, b_\theta)$ which satisfies Assumption 3.

C. Stability Analysis of Complex Gaits

This section addresses the existence and stability of periodic orbits for the cooperative locomotion of the robot and human in the presence of leash. For future purposes, we let Σ^c denote the augmented closed-loop system with the local controllers in Sections III-A and III-B.

***Theorem** 1 (Stability of Complex Gaits with Leash):* Under Assumptions 1-3, there is an open neighborhood of 0, denoted by $\mathcal{N}(0)$, such that for all gain values $\kappa \in \mathcal{N}(0)$, there is an exponentially stable complex gait for Σ^c.

Proof: From Assumptions 1 and 2, the augmented orbit $\mathcal{O}^c_{\text{ul}} := \{x^c = \text{col}(x^d_\star(t), x^h_\star(t)) \,|\, 0 \leq t < N^d_{\min} T^d\}$ is indeed a periodic orbit for the complex and unleashed hybrid system Σ^c. We next choose a Poincaré section transversal to this orbit, denoted by $\mathscr{S}$, and consider a Poincaré return map for Σ^c from $\mathscr{S}$ back to $\mathscr{S}$ as $P^c(x^c, \kappa)$. According to the construction procedure, there is a fixed point for the Poincaré map that corresponds to $\mathcal{O}^c_{\text{ul}}$, that is $P^c(x^c_{\star,\text{ul}}, 0) = x^c_{\star,\text{ul}}$, in which $x^c_{\star,\text{ul}}$ represents the fixed point. We next consider the algebraic equation $E(x^c, \kappa) := P^c(x^c, \kappa) - x^c = 0$. Since $\mathcal{O}^c_{\text{ul}}$ is exponentially stable for the unleashed complex system, the Jacobian matrix $\frac{\partial E}{\partial x^c}(x^c_{\star,\text{ul}}, 0) = \frac{\partial P^c}{\partial x^c}(x^c_{\star,\text{ul}}, 0) - I$ is nonsingular. Hence, from the Implicit Function Theorem, there exists $\mathcal{N}(0)$ such that for all $\kappa \in \mathcal{N}(0)$, there is a fixed point

This article has been accepted for publication in a future issue of this journal, but has not been fully edited. Content may change prior to final publication. Citation information: DOI 10.1109/LRA.2019.2939719, IEEE Robotics and Automation Letters

for $P^c(x^c,\kappa)$. Moreover, since the elements and eigenvalues of the Jacobian matrix $\frac{\partial P^c}{\partial x^c}(x^c,\kappa)$ continuously depend on κ, one can choose $\mathcal{N}(0)$ sufficiently small such that the eigenvalues of the Jacobian matrix remain inside the unit circle. ■

IV. LOCAL VIRTUAL CONSTRAINT CONTROLLERS WITH FORCE FEEDBACK

The objective of this section is to design the local controller for the robotic dog. The controller is designed based on virtual constraints approach [10], [11] to ensure exponential stability of the gait for the unleashed case. Virtual constraints are defined as kinematic constraints (i.e., outputs) that encode the locomotion pattern. They are imposed through the action of the local controllers. We make use of relative degree one and relative degree two virtual constraints (i.e., outputs). In particular, during the continuous-time domain $v \in \mathcal{V}^d$, we consider the outputs $y_v^d(x^d) := \text{col}(y_{1v}^d(q^d,\dot{q}^d), y_{2v}^d(q^d))$ to be regulated, in which $y_{1v}^d(q^d,\dot{q}^d)$ represents relative degree one nonholonomic outputs for velocity regulation and and $y_{2v}^d(q^d)$ denotes relative degree two holonomic outputs for position tracking. Using the nonlinear dynamics (3) and standard input-output linearization [35], one can obtain

$$\text{col}\left(\dot{y}_{1v}^d, \ddot{y}_{2v}^d\right) = A_v^d\left(x^d\right)u^d + b_v^d\left(x^d, F\right), \tag{5}$$

where $A_v^d(x)$ is a decoupling matrix and b_v^d consists of Lie derivatives (see [28] for more details). Furthermore, we would like to solve for u^d that results in

$$\begin{bmatrix}\dot{y}_{1v}^d\\ \ddot{y}_{2v}^d\end{bmatrix} = -\ell_v(x^d) := -\begin{bmatrix}K_P\, y_{1d}^v\\ K_D\,\dot{y}_{2v}^d + K_P\, y_{2v}^d\end{bmatrix} \tag{6}$$

with K_P and K_D being positive-definite PD gains. The local controller for the dog is finally chosen as

$$\Gamma_v^d\left(x^d, F\right) := -A_v^{d\top}\left(A_v^d\, A_v^{d\top}\right)^{-1}\left(b_v^d + \ell_v\right) \tag{7}$$

that 1) requires local state and force measurement and 2) exponentially stabilizes the origin for the output dynamics (6) in the presence of the external force, i.e., $\lim_{t\to\infty} y_v^d(t) = 0$.

***Remark** 2 (Proper Selection of Virtual Constraints):* For a given periodic gait $\mathcal{O}_{\text{ul}}^d$, the output functions y_v^d are chosen to vanish on $\mathcal{O}_{\text{ul}}^d$. We have observed that the stability of gaits in the virtual constraint approach depends on the proper selection of the output functions y_v^d to be regulated [29]. Our previous work [29], [30] has developed a recursive optimization algorithm to systematically design output functions for which the gaits are exponentially stable for the hybrid dynamics. The algorithm is offline and assumes a finite-dimensional parameterization of the output functions to be determined. Then it translates the exponential stabilization problem into a recursive optimization problem involving linear and bilinear matrix inequalities.

***Remark** 3:* Nonlinear local controllers for the human model are not known. However, for the purpose of this paper, we assume virtual constraint-based controllers, analogous to (7), for the human model. Furthermore, evidence suggests that the phase-dependent models can reasonably predict human joint behavior across perturbations [36].

V. QP FOR SAFETY-CRITICAL CONTROL

This section aims to develop low-level safety-critical control algorithms that ensure obstacle avoidance while implementing the local controllers. We will address safety critical conditions through set invariance and CBFs. In particular, a system being safe is commonly defined as the system never leaving the safety set [25], [26], [27]. We make use of a real-time QP formulation to address safety specifications represented by CBFs [25]. To present the main idea, let us consider a discrete set of static and point obstacles $\mathscr{P}_\alpha^o$ for $\alpha \in \mathcal{I}^o$ whose Cartesian coordinates in the xy-planes are given by $r_\alpha^o := \text{col}(x_\alpha^o, y_\alpha^o)$. Next we assume a set of critical points on the robot and human that are supposed to be in a safe distance from these obstacles. These points are denoted by $\mathscr{P}_\beta^d$ and $\mathscr{P}_\gamma^h$ for the dog and human, respectively, for some $\beta \in \mathcal{I}^d$ and $\gamma \in \mathcal{I}^h$. One typical example includes the hip points of the robot and human models. The Cartesian coordinates of $\mathscr{P}_\beta^d$ and $\mathscr{P}_\gamma^h$ in the xy-plane are further denoted by $r_\beta^d(q^d) \in \mathbb{R}^2$ and $r_\gamma^h(q^h) \in \mathbb{R}^2$. We formulate the safety set as $\mathcal{C} := \{x^c = \text{col}(x^d, x^h) \,|\, h_{\beta,\alpha}^d(q^d) \geq 0,\, h_{\gamma,\alpha}^h(q^h) \geq 0, \forall(\alpha,\beta,\gamma) \in \mathcal{I}^o \times \mathcal{I}^d \times \mathcal{I}^h\}$, where $h_{\beta,\alpha}^d(q^d) := \|r_\beta^d(q^d) - r_\alpha^o\|_2^2 - h_{\min}^2$ and $h_{\gamma,\alpha}^h(q^h) := \|r_\gamma^h(q^h) - r_\alpha^o\|_2^2 - h_{\min}^2$ for some safety distance $h_{\min} > 0$. The safety constraints $h_{\beta,\alpha}^d(q^d) \geq 0$ and $h_{\gamma,\alpha}^h(q^h) \geq 0$ are relative degree two. Our objective is to modify the torques for the dog robot u^d as well as the leash force F to render the safety set $\mathcal{C}$ forward invariant under the flow of the closed-loop complex model. We remark that we are *not* allowed to change the human controller $u^h = \Gamma^h(x^h, F)$ as the person can be visually impaired and cannot react properly. For this purpose, we make use of the concept of exponential CBFs (ECBFs) [37]. In particular, we define the ECBFs as follows

$$\mathcal{B}_{\beta,\alpha}^d\left(x^d\right) := \dot{h}_{\beta,\alpha}^d\left(x^d\right) + \lambda\, h_{\beta,\alpha}^d\left(x^d\right) \tag{8}$$

$$\mathcal{B}_{\gamma,\alpha}^h\left(x^h\right) := \dot{h}_{\gamma,\alpha}^h\left(x^h\right) + \lambda\, h_{\gamma,\alpha}^h\left(x^h\right) \tag{9}$$

for all $(\alpha,\beta,\gamma) \in \mathcal{I}^o \times \mathcal{I}^d \times \mathcal{I}^h =: \mathcal{I}$, where $\lambda > 0$ is an adjustable parameter. The exponential CBF condition further implies that $\dot{\mathcal{B}}_{\beta,\alpha}^d(x^d,u^d,F) + \omega\,\mathcal{B}_{\beta,\alpha}(x^d) \geq 0$ and $\dot{\mathcal{B}}_{\gamma,\alpha}^h(x^h,F) + \omega\,\mathcal{B}_{\gamma,\alpha}(x^h) \geq 0$ for all $(\alpha,\beta,\gamma) \in \mathcal{I}$ and some adjustable scalar $\omega > 0$. This results in $\ddot{h}_{\beta,\alpha}^d + (\lambda+\omega)\,\dot{h}_{\beta,\alpha}^d + \lambda\,\omega\, h_{\beta,\alpha}^d \geq 0$ and $\ddot{h}_{\gamma,\alpha}^h + (\lambda+\omega)\,\dot{h}_{\gamma,\alpha}^h + \lambda\,\omega\, h_{\gamma,\alpha}^h \geq 0$. From (3), these lateral inequalities can be expressed as affine inequalities in terms of (u^d, F), i.e.,

$$A_{\beta,\alpha}^d\left(x^d\right)\text{col}\left(u^d, F\right) + b_{\beta,\alpha}^d\left(x^d\right) \geq 0 \tag{10}$$

$$A_{\gamma,\alpha}^h\left(x^h\right)F + b_{\gamma,\alpha}^h\left(x^h\right) \geq 0 \tag{11}$$

for all $(\alpha,\beta,\gamma) \in \mathcal{I}$. Next, we set up the following real-time QP to ensure safety-critical constraints while being close to the local controllers

$$\begin{aligned}\min_{(u^d,F)}\quad & \left\|u^d - \Gamma^d\left(x^d,F\right)\right\|_2^2 + \left\|F - F_b\left(r,\dot{r},\theta,\dot{\theta},\kappa\right)\right\|_2^2\\ \text{s.t.}\quad & A_{\beta,\alpha}^d\left(x^d\right)\begin{bmatrix}u^d\\ F\end{bmatrix} + b_{\beta,\alpha}^d\left(x^d\right) \geq 0,\ \forall(\alpha,\beta,\gamma) \in \mathcal{I}\\ & A_{\gamma,\alpha}^h\left(x^h\right)F + b_{\gamma,\alpha}^h\left(x^h\right) \geq 0, \quad \forall(\alpha,\beta,\gamma) \in \mathcal{I}\\ & u_{\min} \leq u^d \leq u_{\max}, \quad F_{\min} \leq F \leq F_{\max},\end{aligned} \tag{12}$$

This article has been accepted for publication in a future issue of this journal, but has not been fully edited. Content may change prior to final publication. Citation information: DOI 10.1109/LRA.2019.2939719, IEEE Robotics and Automation Letters

where $u_{\min}$, $u_{\max}$, $F_{\min}$, and $F_{\max}$ denote the lower and upper bounds for the torques and forces. We remark that according to the construction procedure of the local controller in (5) and (7), $b_v^d(x^d, F)$ and $\Gamma_v^d(x^d, F)$ are affine in terms of the leash force F for every $v \in \mathcal{V}^d$. Hence, the cost function in (12) is indeed quadratic in terms of (u^d, F).

Remark 4: In the QP formulation (12), one would need to asymptotically estimate the human state variables x^h to check for the constraints (11). This assumption is not restrictive. In particular, our previous work [38] has developed asymptotic observers to estimate the state variables for 3D human models via a set of wearable inertial measurement units (IMUs) attached to the links (e.g., torso, tibia, and femur). Alternative observer design approaches for bipedal locomotion have been developed in the literature, e.g., [39], [40], which validates the feasibility of this assumption.

Remark 5: If the QP in (12) is not feasible for a time sample, one may employ the local controllers $\Gamma^d(x^d, F)$ and $F_b(r, \dot{r}, \theta, \dot{\theta}, \kappa)$ (i.e., higher-level control) for the dog and leash structure, respectively. From (3), it is easy to show that $A^d_{\beta,\alpha}(x^d) = 2(r^d_\beta - r^o_\alpha)\, J^d_\beta\, (D^d)^{-1}\, [T^d_v \;\; - J^{d\top}_{\text{head}}]$, where $J^d_\beta := \partial r^d_\beta / \partial q^d$. Consequently, if the safety critical point r^d_β on the robot is sufficiently close to the object r^o_α, then $A^d_{\beta,\alpha}$ may not be full-rank. This may happen for steep curvatures and result in infeasibility of the QP. Consequently, the proposed approach can "locally" modify the pre-designed robot and human trajectories to avoid obstacles.

Remark 6: The output of the QP is indeed used at the actuator and joint levels. The higher-level control is synthesized with offline optimization algorithm as mentioned in Remark 2, while the lower-level control is synthesized via the online QP. This makes the control strategy a hierarchical policy. The higher-level is for the stability, and the lower-level is for modification in case of obstacles.

VI. NUMERICAL SIMULATIONS AND RESULTS

The objective of this section is to numerically validate the theoretical results of the paper. For this purpose, we consider a complex and full-order hybrid dynamical model that describes the cooperative locomotion of Vision 60 and a human model. Vision 60 is an autonomous quadrupedal robot manufactured by Ghost Robotics [6]. It weighs approximately 26 kg with 18 DOFs. More specifically, each leg of the robot consists of a 1 DOF actuated knee joint with pitch motion and a 2 DOF actuated hip joint with pitch and roll motions. In addition, 6 DOFs are associated with the translational and rotational motions of the torso. The human model consists of a rigid tree structure with a torso link, including hands and head, and two identical legs terminating at point feet (see [30]). Each leg of the robot includes 3 actuated joints: a 2 DOF hip (ball) joint with roll and pitch motions and a 1 DOF knee joint. The model has 12 DOFs: 6 DOF for the translational and rotational motions of the torso and 6 DOF for the internal shape variables. The kinematic and dynamic parameter are taken according to those reported in [41] from a human cadaver study.

Path Planning: We consider an unleashed trotting gait $\mathcal{O}^d_{\text{ul}}$ for the dog robot at the speed of 1.2 (m/s). To generate the gait, we make use of FROST (Fast Robot Optimization and Simulation Toolkit) — an open-source toolkit for path planning of dynamic legged locomotion [42], [14]. FROST makes use of the Hermite-Simpson collocation approach to translate the path planning problem into a nonlinear programming (NLP) that can be effectively solved with state-of-the-art NLP tools such as IPOPT. Two periodic bipedal gaits $\mathcal{O}^h_{\text{ul}}$ are designed for the locomotion of the human model at the speeds of 1.1 (m/s) and 1.3 (m/s). We intentionally design two gaits, one slower and the other faster than that of the dog, to show that the proposed control strategy results in a common speed leashed gait for both scenarios.

Local Controllers: Using the optimization algorithm of [29], [30], we synthesize the virtual constraint controllers of (7) in an offline manner to exponentially stabilize the unleashed gaits for the dog and human models. We further do not consider the full state stability for the human gait. Instead, we consider the *stability modulo yaw* [29, Section 6.5] to have a model of visually impaired people locomotion. We remark that the dog robot together with the leash structure will have the responsibility to stabilize the yaw motion for itself as well as the human. The leash local controller is further designed to keep the human in the safe zone of $[1.25, 1.8]$ (m). Figures 4a and 4b depict the robot and human center of mass (COM) trajectories in the xy-plane without and with using the leash structure, respectively. Here, we make use of the slower gait for the human. We remark that without the leash, the human gait does *not* have the yaw stability (see Fig. 4a). However, utilizing the leash structure, the robot and human trajectories converge to a complex gait with the same speed while having the yaw stability (see Fig. 4b).

Obstacle Avoidance: We consider a set of point obstacles $\mathscr{P}^o_\alpha$ for some α in the discrete set $\mathcal{I}^o$. The critical points on the robot and human (i.e., $\mathscr{P}^d_\beta$ and $\mathscr{P}^h_\gamma$) are then chosen as the hip points. For both the slower (i.e., 1.1 (m/s)) and faster (i.e., 1.3 (m/s)) unleashed gaits of the human, we consider 18 obstacles around the steady-state trajectories. In both scenarios, the unleashed gait for the dog has the speed of 1.2 (m/s). Without employing the real-time QP-based modification, the robot and human COM can hit the obstacles. In particular, Fig. 4b illustrates an undershoot around -0.3 (m) along the y-axis for the human COM that can easily collide with the obstacle located there in Fig. 4c. However, utilizing the hierarchical control algorithm with QP running at 1kHz, the robot and human trajectories are locally modified around the steady-state gait such that the safety critical conditions are satisfied (see Figs. 4c and 5a for the simulated scenarios with slow and fast gaits of the human, respectively.). The numerical results show that using the proposed approach, the human model can adapt to the guide dog whose speed and heading direction are in the rang of $\pm 10\%$ of the human's speed and $[-\frac{\pi}{6}, \frac{\pi}{6}]$ (rad), respectively. The time profile of (r, θ) as well as the optimized (F_r, F_θ) generated by QP to accommodate the obstacles of Fig. 4c is depicted in Figs. 5b and 5c, respectively. We observe that the peak values for F_r and F_θ are 12 (N) and 20 (N), respectively, which results in the peak value for the torque $\tau = r\, F_\theta$ as 42 (Nm). This range of data validates the feasibility of implementing the proposed control approach in

This article has been accepted for publication in a future issue of this journal, but has not been fully edited. Content may change prior to final publication. Citation information: DOI 10.1109/LRA.2019.2939719, IEEE Robotics and Automation Letters

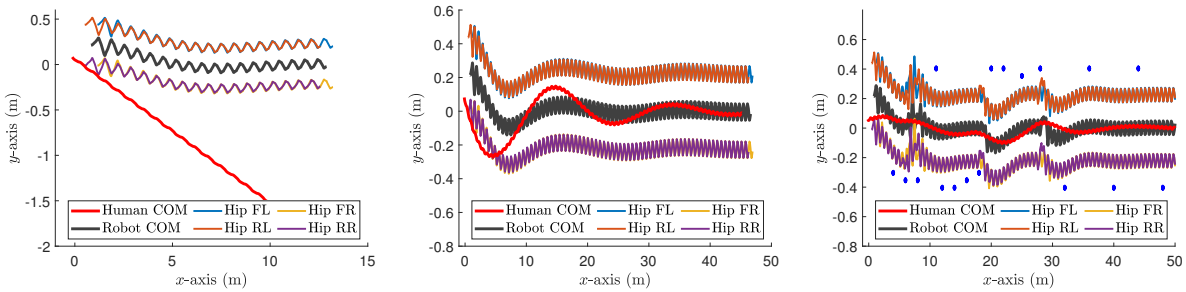

(a) (b) (c)

Fig. 4: (a) Robot and human COM trajectories in the xy-plane without using the leash structure. The unleashed gait for the dog is exponentially stable (i.e, it walks along a line parallel to the x-axis on which the yaw angle is zero). However, the one for the human is modulo yaw stable. The unleashed gaits for the dog and human have the speed of 1.1 (m/s) and 1.2 (m/s), respectively. (b) COM trajectories using the leash structure. Here the leash and each agent have its own local controllers and there is *no* CBF-based QP optimization. Both the robot and human converge to a complex gait with a common speed while having yaw stability. (c) COM trajectories using the proposed hierarchical control strategy in the presence of point obstacles. The obstacles are illustrated by the circles.

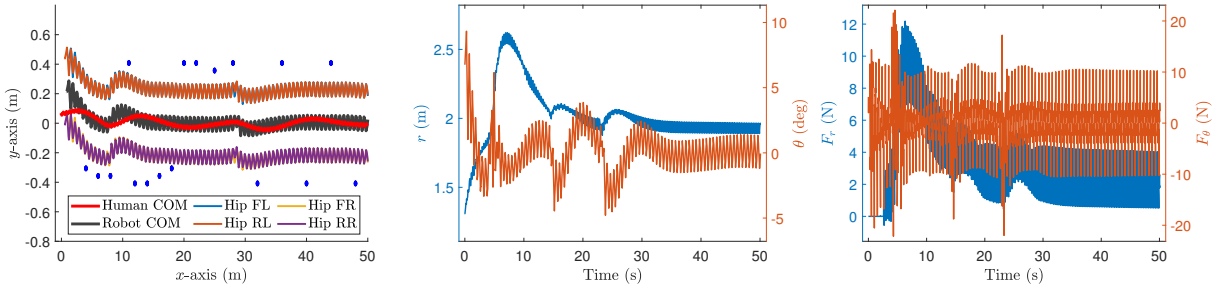

(a) (b) (c)

Fig. 5: (a) COM trajectories using the proposed hierarchical control strategy for the case in which the unleashed gaits for the dog and human have the speed of 1.2 (m/s) and 1.3 (m/s), respectively. Both agents reach a common speed. (b) Time profiles of r and θ using the proposed hierarchical control strategy in the simulation of Fig. 4c. (c) Time profiles of the modified longitudinal and torsional forces F_r and F_θ generated by the QP optimization for obstacle avoidance in Fig. 4c.

reality. Figure 6 finally illustrates the snapshots of the robot and human locomotion around the obstacles. Animations can be found online [43].

VII. CONCLUSION

This paper presented a formal method towards 1) addressing complex hybrid dynamical models that describe cooperative locomotion of guide legged robots and humans and 2) systematically designing hierarchical control algorithms that enable stable and safe collaborative locomotion in the presence of discrete obstacles. At the higher level of the proposed control strategy, local controllers are assumed for the robotic dog and the leash structure. The robot local controller is developed based on HZD approach to asymptotically stabilize a predesigned unleashed gait for the quadrupedal robot. The leash local controller is further developed to keep the human in a safe distance from the dog while following it. The existence and exponential stability of leashed gaits for the complex model are investigated via the Poincaré return map. At the lower level, a real-time QP is solved to modify the local controllers for the robot as well as the leash to ensure safety (i.e., obstacles avoidance) via CBFs. The power of the analytical approach is validated through extensive numerical simulations of a complex hybrid model with 60 state variables and 20 control inputs that represents the cooperative locomotion of Vision 60 and a human model. We considered an unleashed trotting gait for the dog and two bipedal gaits for the human. It is shown that using the proposed control strategy, the dog and human can reach a common speed for the leashed motion. Moreover, we demonstrated that the robot can stabilize the yaw motion for the human model. The proposed approach can locally guarantee safety around pre-designed unleashed trajectories. For future research, we will improve control algorithms to address sharp turns around corners and obstacles. We will also investigate robust hierarchical approaches to address cooperative locomotion over uneven terrains.

REFERENCES

[1] Perkins School for the Blind, https://www.perkins.org/stories/10-fascinating-facts-about-the-white-cane.

[2] P. J. Craigon, P. Hobson-West, G. C. W. England, C. Whelan, E. Lethbridge, and L. Asher, "She's a dog at the end of the day: Guide dog owners' perspectives on the behaviour of their guide dog," *PLOS ONE*, vol. 12, no. 4, pp. 1–19, 04 2017. [Online]. Available: https://doi.org/10.1371/journal.pone.0176018

[3] S. Kayukawa, K. Higuchi, J. Guerreiro, S. Morishima, Y. Sato, K. Kitani, and C. Asakawa, "Bbeep: A sonic collision avoidance system for blind travellers and nearby pedestrians," 05 2019.

[4] E. Ohn-Bar, J. a. Guerreiro, K. Kitani, and C. Asakawa, "Variability in reactions to instructional guidance during smartphone-based assisted navigation of blind users," *Proc. ACM Interact. Mob. Wearable Ubiquitous Technol.*, vol. 2, no. 3, pp. 131:1–131:25, Sep. 2018. [Online]. Available: http://doi.acm.org/10.1145/3264941

[5] D. Sato, U. Oh, K. Naito, H. Takagi, K. Kitani, and C. Asakawa, "NavCog3: An evaluation of a smartphone-based blind indoor navigation

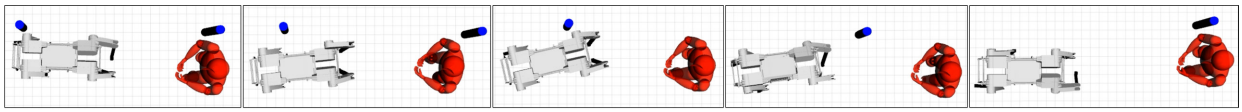

(a) (b) (c) (d) (e)

Fig. 6: Simulation snapshots illustrating the evolution ((a) to (e)) of Vision 60 and human trajectories on having a close encounter with the obstacles. The visualization does not illustrate the actuated leash. However, it's effect is clearly demonstrated by the augmented human trajectory in figures (see [43] for the animation).

assistant with semantic features in a large-scale environment," 10 2017, pp. 270–279.

[6] Ghost Robotics, https://www.ghostrobotics.io/.

[7] T. Chuang, N. Lin, J. Chen, C. Hung, Y. Huang, C. Tengl, H. Huang, L. Yu, L. Giarr, and H. Wang, "Deep trail-following robotic guide dog in pedestrian environments for people who are blind and visually impaired - learning from virtual and real worlds," in *2018 IEEE International Conference on Robotics and Automation (ICRA)*, May 2018, pp. 1–7.

[8] J. E. Young, Y. Kamiyama, J. Reichenbach, T. Igarashi, and E. Sharlin, "How to walk a robot: A dog-leash human-robot interface," in *2011 RO-MAN*, July 2011, pp. 376–382.

[9] I. Ulrich and J. Borenstein, "The guidecane-applying mobile robot technologies to assist the visually impaired," *IEEE Transactions on Systems, Man, and Cybernetics - Part A: Systems and Humans*, vol. 31, no. 2, pp. 131–136, March 2001.

[10] J. Grizzle, G. Abba, and F. Plestan, "Asymptotically stable walking for biped robots: Analysis via systems with impulse effects," *Automatic Control, IEEE Transactions on*, vol. 46, no. 1, pp. 51–64, Jan 2001.

[11] E. Westervelt, J. Grizzle, and D. Koditschek, "Hybrid zero dynamics of planar biped walkers," *Automatic Control, IEEE Transactions on*, vol. 48, no. 1, pp. 42–56, Jan 2003.

[12] C. Chevallereau, J. Grizzle, and C.-L. Shih, "Asymptotically stable walking of a five-link underactuated 3-D bipedal robot," *Robotics, IEEE Transactions on*, vol. 25, no. 1, pp. 37–50, Feb 2009.

[13] A. Ames, K. Galloway, K. Sreenath, and J. Grizzle, "Rapidly exponentially stabilizing control Lyapunov functions and hybrid zero dynamics," *Automatic Control, IEEE Transactions on*, vol. 59, no. 4, pp. 876–891, April 2014.

[14] A. Hereid, C. M. Hubicki, E. A. Cousineau, and A. D. Ames, "Dynamic humanoid locomotion: A scalable formulation for HZD gait optimization," *IEEE Transactions on Robotics*, pp. 1–18, 2018.

[15] K. Sreenath, H.-W. Park, I. Poulakakis, and J. W. Grizzle, "Compliant hybrid zero dynamics controller for achieving stable, efficient and fast bipedal walking on MABEL," *The International Journal of Robotics Research*, vol. 30, no. 9, pp. 1170–1193, Aug. 2011.

[16] H.-W. Park, A. Ramezani, and J. Grizzle, "A finite-state machine for accommodating unexpected large ground-height variations in bipedal robot walking," *Robotics, IEEE Transactions on*, vol. 29, no. 2, pp. 331–345, April 2013.

[17] I. Poulakakis and J. Grizzle, "The spring loaded inverted pendulum as the hybrid zero dynamics of an asymmetric hopper," *Automatic Control, IEEE Transactions on*, vol. 54, no. 8, pp. 1779–1793, Aug 2009.

[18] H. Dai and R. Tedrake, "Optimizing robust limit cycles for legged locomotion on unknown terrain," in *Decision and Control, IEEE 51st Annual Conference on*, Dec 2012, pp. 1207–1213.

[19] C. O. Saglam and K. Byl, "Meshing hybrid zero dynamics for rough terrain walking," in *2015 IEEE International Conference on Robotics and Automation (ICRA)*, May 2015, pp. 5718–5725.

[20] A. M. Johnson, S. A. Burden, and D. E. Koditschek, "A hybrid systems model for simple manipulation and self-manipulation systems," *The International Journal of Robotics Research*, vol. 35, no. 11, pp. 1354–1392, 2016.

[21] M. Spong and F. Bullo, "Controlled symmetries and passive walking," *Automatic Control, IEEE Transactions on*, vol. 50, no. 7, pp. 1025–1031, July 2005.

[22] I. Manchester, U. Mettin, F. Iida, and R. Tedrake, "Stable dynamic walking over uneven terrain," *The International Journal of Robotics Research*, vol. 30, no. 3, pp. 265–279, 2011.

[23] R. Vasudevan, *Hybrid System Identification via Switched System Optimal Control for Bipedal Robotic Walking*. Cham: Springer International Publishing, 2017, pp. 635–650.

[24] A. D. Ames, R. D. Gregg, E. D. B. Wendel, and S. Sastry, "On the geometric reduction of controlled three-dimensional bipedal robotic walkers," in *Lagrangian and Hamiltonian Methods for Nonlinear Control 2006*. Berlin, Heidelberg: Springer Berlin Heidelberg, 2007, pp. 183–196.

[25] A. D. Ames, X. Xu, J. W. Grizzle, and P. Tabuada, "Control barrier function based quadratic programs for safety critical systems," *IEEE Transactions on Automatic Control*, vol. 62, no. 8, pp. 3861–3876, 2017. [Online]. Available: http://ames.caltech.edu/ames2017cbf.pdf

[26] T. Gurriet, M. Mote, A. D. Ames, and E. Feron, "An online approach to set invariance," To appear in IEEE Conference on Decision and Control (CDC), 2018. [Online]. Available: http://ames.caltech.edu/gurriet2018online.pdf

[27] Q. Nguyen, A. Hereid, J. W. Grizzle, A. D. Ames, and K. Sreenath, "3d dynamic walking on stepping stones with control barrier functions," in *2016 IEEE 55th Conference on Decision and Control (CDC)*, Dec 2016, pp. 827–834.

[28] K. Akbari Hamed, W. Ma, and A. D. Ames, "Dynamically stable 3D quadrupedal walking with multi-domain hybrid system models and virtual constraint controllers," in *American Control Conference, arXiv preprint arXiv:1810.06697*, July Accepted to Appear, 2019. [Online]. Available: https://arxiv.org/abs/1810.06697

[29] K. Akbari Hamed, B. Buss, and J. Grizzle, "Exponentially stabilizing continuous-time controllers for periodic orbits of hybrid systems: Application to bipedal locomotion with ground height variations," *The International Journal of Robotics Research*, vol. 35, no. 8, pp. 977–999, 2016.

[30] K. Akbari Hamed and R. D. Gregg, "Decentralized feedback controllers for robust stabilization of periodic orbits of hybrid systems: Application to bipedal walking," *Control Systems Technology, IEEE Transactions on*, vol. 25, no. 4, pp. 1153–1167, July 2017.

[31] S. Veer, M. S. Motahar, and I. Poulakakis, "Adaptation of limit-cycle walkers for collaborative tasks: A supervisory switching control approach," in *2017 IEEE/RSJ International Conference on Intelligent Robots and Systems (IROS)*, Sep. 2017, pp. 5840–5845.

[32] ——, "On the adaptation of dynamic walking to persistent external forcing using hybrid zero dynamics control," in *2015 IEEE/RSJ International Conference on Intelligent Robots and Systems (IROS)*, Sep. 2015, pp. 997–1003.

[33] S. Veer and I. Poulakakis, "Safe adaptive switching among dynamical movement primitives: Application to 3D limit-cycle walkers.," *arXiv preprint arXiv:1810.00527*, 2019.

[34] Y. Hurmuzlu and D. B. Marghitu, "Rigid body collisions of planar kinematic chains with multiple contact points," *The International Journal of Robotics Research*, vol. 13, no. 1, pp. 82–92, 1994.

[35] A. Isidori, *Nonlinear Control Systems*. Springer; 3rd edition, 1995.

[36] D. J. Villarreal, H. A. Poonawala, and R. D. Gregg, "A robust parameterization of human gait patterns across phase-shifting perturbations," *IEEE Transactions on Neural Systems and Rehabilitation Engineering*, vol. 25, no. 3, pp. 265–278, March 2017.

[37] Q. Nguyen and K. Sreenath, "Exponential control barrier functions for enforcing high relative-degree safety-critical constraints," in *2016 American Control Conference (ACC)*, July 2016, pp. 322–328.

[38] K. Akbari Hamed, A. Ames, and R. Gregg, "Observer-based feedback controllers for exponential stabilization of hybrid periodic orbits: Application to underactuated bipedal walking," in *2018 Annual American Control Conference (ACC)*, June 2018, pp. 1438–1445.

[39] V. Lebastard, Y. Aoustin, and F. Plestan, "Observer-based control of a walking biped robot without orientation measurement," *Robotica*, vol. 24, no. 3, pp. 385–400, May 2006.

[40] J. W. Grizzle, J. H. Choi, H. Hammouri, and B. Morris, "On observer-based feedback stabilization of periodic orbits in bipedal locomotion," in *Methods and Models in Automation and Robotics*, August 2007, pp. 27–30.

[41] P. de Leva, "Adjustments to Zatsiorsky-Seluyanov's segment inertia parameters," *J Biomech*, vol. 29, no. 9, pp. 123–1230, 1996.

[42] A. Hereid and A. D. Ames, "FROST: Fast robot optimization and simulation toolkit," in *2017 IEEE/RSJ International Conference on Intelligent Robots and Systems (IROS)*, Sept 2017, pp. 719–726.

[43] Hierarchical and Safe Motion Control for Cooperative Human-Robot Locomotion, https://youtu.be/nV2prm5Imbs.